Journal of Process Control 27 (2015) 76–86

Contents lists available at ScienceDirect

Journal of Process Control

journal homepage: www.elsevier.com/locate/jprocont

On control of transport in Brownian ratchet mechanisms

Subhrajit Roychowdhury[a,*], Govind Saraswat[a], Srinivasa Salapaka[b], Murti Salapaka[a]

[a] Department of Electrical and Computer Engineering, University of Minnesota-Twin Cities, 2-270 Keller Hall, Minneapolis, MN 55455, USA
[b] Department of Mechanical Science and Engineering, University of Illinois at Urbana-Champaign, 1206 West Green Street, Urbana, IL 61801, USA

ARTICLE INFO

Article history:
Received 1 April 2014
Received in revised form
15 September 2014
Accepted 26 November 2014
Available online 23 December 2014

Keywords:
Flashing ratchet
Stochastic systems
Dynamic programming
Optimization
Colloidal self-assembly

ABSTRACT

Engineered transport of material at the nano/micro scale is essential for the manufacturing platforms of the future. Unlike conventional transport systems, at the nano/micro scale, transport has to be achieved in the presence of fundamental sources of uncertainty such as thermal noise. Remarkably, it is possible to extract useful work by rectifying noise using an asymmetric potential; a principle used by Brownian ratchets. In this article a systematic methodology for designing open-loop Brownian ratchet mechanisms that optimize velocity and efficiency is developed. In the case where the particle position is available as a measured variable, closed loop methodologies are studied. Here, it is shown that methods that strive to optimize velocity of transport may compromise efficiency. A dynamic programming based approach is presented which yields up to three times improvement in efficiency over optimized open loop designs and 35% better efficiency over reported closed loop strategies that focus on optimizing velocities.

1. Introduction

Engineered nanoscale systems are posed to enable high efficiency and unparalleled precision in specificity in fabrication and manufacturing of materials and structures. Such a capability can result in new materials and devices with a vast range of applications in diverse areas such as medicine, electronics, and bio-materials [2,16,17,19,25]. The success of such a paradigm critically rests on the quality of transport of micro/nanoscale components from sources to destinations. An associated goal is the differentiation of components into separate groups based on different properties. Key insights on engineering transport mechanisms can be obtained from how biology utilizes micro/nano scale objects to achieve macro scale functionality. For example, in eukaryotic cells, material is transported on microtubular networks by motor proteins (kinesin and dynein) [11,26]; a detailed understanding of the underlying transport mechanisms can play a significant role in realizing productive engineered transport systems at the molecular scale. Use of biological constructs to realize such systems has found recent focus [7,23,27]. However, considerable challenges remain on both the fundamental understanding of transport mechanisms at the molecular scale and related engineering tasks.

A significant challenge for realizing efficient transport at the nano/molecular scale is posed by noise. Unlike in macroscale systems, *thermal noise* that causes Brownian motion often determines the limits of performance of molecular scale systems. For example, a kinesin motor protein (which together with dynein carry cargo inside a cell) moves on microtubules (MTs) with a characteristic step length of 8 nm; the motion caused by thermal noise has similar magnitude of standard deviations and thus a kinesin molecule has to achieve robust transport under a significant source of noise.

Remarkably, there are mechanisms that take advantage of Brownian motion to achieve directed motion. In the presence of Brownian motion, *Brownian ratchet* mechanisms use spatially periodic potential that are alternately turned on and off, to realize transport in preferred directions. For achieving the preferential bias in the motion, it is essential that the potential be asymmetric within the period; similar to the potential in a ratchet-and-pawl mechanism [10]. Moreover, in *Brownian ratchet* mechanisms, without the Brownian motion, no mean movement of particles is possible [2,18]; thus here Brownian motion is indeed an enabling factor. In many naturally occurring systems the potential is realized only at the vicinity of the moving entity, thus being more efficient [1].

In many engineered realizations where noise is marshaled for enabling motion in a desired direction, a spatially periodic potential is realized over the whole extent of the transport regime. The resulting mechanisms are also used to separate different constituents of a mixture by exploiting the dependence of diffusion constants on

* Corresponding author. Tel.: +1 6125985316.
E-mail address: subhra@umn.edu (S. Roychowdhury).

http://dx.doi.org/10.1016/j.jprocont.2014.11.012
0959-1524/

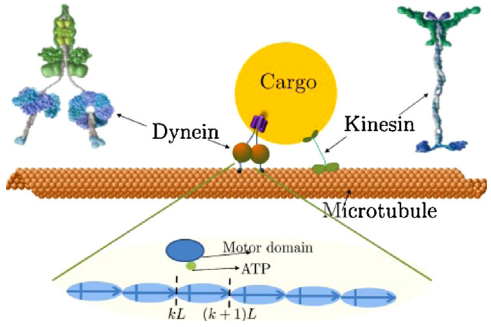

Fig. 1. The top schematic shows the transport of a cargo by motor proteins Kinesin and Dynein that *walk* on linear lattice provided by microtubules (MT). A simple model of MT is a linear arrangement of dipole moments (which is shown in the bottom figure). When an ATP/ADP molecule (which has a charge) is attached to the motor domain, the motor protein will feel the electrostatic force due to the dipole moments which depends on whether an ATP or an ADP is attached. The string of dipole moments provides the periodic asymmetric potential and the acquisition and loss of ATP/ADP switches the ratchet potential. It is possible that the rate of switching between the ADP and ATP molecules is dependent on where the motor domain is with respect to the MT unit that is modeled as a dipole. It is postulated that due to conformational changes in the motor protein structure, ATP/ADP exchange rate is different in the first α fraction of the dipole length in comparison to the case when the motor domain is anywhere in the rest of the $1-\alpha$ fraction.

physical properties (such as size) which results in different transport velocities. A flashing ratchet potential can also be realized, for example, using periodically asymmetric and transversely interleaved geometric patterns etched on surfaces and using electric fields in the transverse direction of motion (see geometric ratchets in [16,25]). In many applications only open-loop strategies are viable; for example, in geometric ratchets, the patterns are fixed and cannot be altered in real-time. Also, open-loop strategies have significant relevance when transport of many dispersed particles is involved. In open loop strategies a key design issue is to determine the on-and-off time schedule for the potential which optimizes transport efficiency and time to destination. Results in this article enable determination of optimal open-loop schedules that yield maximum efficiency/velocity for a given physical system without resorting to exhaustive Monte Carlo methods. In particular, the *stalling force* that prohibits appreciable forward transport, schedules that severely limit forward transport and schedules that result in non-negligible forward transport are determined. The viable range of on–off schedules are used to obtain bounds on forward and backward transport that can occur in a single on–off cycle, which are used to obtain an analytical estimate of the probability density function of the particle position. Error bounds on the estimated pdf of the position from the true pdf are obtained. The analysis and results above provide critical guidance in the design of ratchet mechanisms, which will lead to better transport mechanisms in applications, for example, in colloidal self-assembly [16,25] and separation of mixtures [2].

Closed-loop strategies hold significant promise of increasing transport efficiency in Brownian ratchet based mechansms. As alluded to earlier, motor-proteins, such as kinesin and dynein carry cargo inside a cell over MT networks (see Fig. 1). Each MT is formed by dimer units, which can be modeled as dipoles. Motor-proteins acquire ATP and ADP molecules that have different charge densities and thus by conversion between these molecules (via hydrolysis) the effective interaction potential between the motor complex and the microtubule is changed. The electrostatic force felt by the motor depends on where the ATP/ADP molecule is in relation to the dimer unit, providing a natural feedback mechanism; and thermal forcing provides the noise component. Thus all the ingredients that constitute a Brownian ratchet, with feedback, are present in the molecular motor based transport [4,22]. Engineered systems can be synthesized and used to study the effect of feedback mechanisms that govern changes in the potential. These studies can be used to develop *efficient* feedback strategies in the transport of a single particle. Although closed-loop strategies are considered in the literature, most focus on maximizing velocity of transport (for example, [9]) and do not consider efficiency ([5] does emphasize importance of transport efficiency). In this article, the trade-off between the average velocity of the particle and the energy required are obtained by solving a multiobjective stochastic optimization problem. It is shown that optimal feedback control strategies can be obtained using a dynamic programming formulation in a tractable manner. Similar approach have been adopted for a flashing ratchet system in [21], although the objective there was limited to maximization of velocity under certain conditions. A key insight obtained is that optimizing average velocity may compromise efficiency. For a given set of physical parameters the study provides guidelines on the choice of velocities to target maximum efficiency. Apart from providing guidance on engineered systems, the study of feedback mechanisms will enable the study of molecular motors, where analytical results can be used to decipher experimental data to assess whether feedback is essential (or the extent to which feedback is needed) to explain the data. Since often for many particle systems, the objectives are cast in terms of the center of mass of the particle positions [5,6], efficient single-particle feedback strategies can prove helpful when applied to a virtual particle at the center of mass of the particle ensemble. The closed-loop performance also provides bound on the limits-of-performance of many particle systems.

The paper is organized as follows: In Section 2, the basic operating principle of flashing ratchets is discussed and a mathematical model is provided. In Section 3, a systematic framework to maximize velocity and efficiency for open-loop operation is developed. In Section 4, the problem of maximizing efficiency is cast as a multiobjective optimization problem, which is converted into a dynamic programming problem. A solution together with an analysis of the computational cost is derived. Simulation results accompany the analysis throughout the article. Finally, the findings of the present work are summarized in Section 5.

2. Principle of operation and modeling

Brownian rectifiers constitute a class of mechanisms that realize transport in a preferential direction via 'rectification' of thermal noise. To understand how a Brownian ratchet rectifies noise to obtain preferential movement of particles, consider a simple version of a ratchet shaped potential (see Fig. 2(a)) that remains on and off in an alternating manner for time intervals t_{on} and t_{off}, respectively.[1] Here the potential is periodic with a period L and has positive slope (the corresponding force, $-(\partial V/\partial x)$, is negative) in the interval $(kL, (k+\alpha)L)$ and a negative slope (the corresponding force is positive) in the interval $((k-1+\alpha)L, kL)$ of the kth spatial period. Consider a particle located at the kth valley at time $t=0$. We represent the dynamics of the particle in terms of the time evolution of the probability density function $p(x, t|x_0 = kL, 0)$, which is the probability of the particle being at position x at time t given that it was at $x = kL$ at time $t = 0$. Thus, $p(x, 0|kL, 0) = \delta(x - kL)$, where $\delta(x)$ is the Dirac-delta function. Suppose the potential is off in the time interval $[0, t_{off}]$; then the motion of the particle is governed by Brownian motion and the pdf is given by (see Fig. 2(b))

$$p(x, t|kL, 0) = \frac{1}{\sqrt{4\pi Dt}} \exp\left(-\frac{(x-kL)^2}{4Dt}\right). \quad (1)$$

[1] And hence the name 'flashing ratchet'

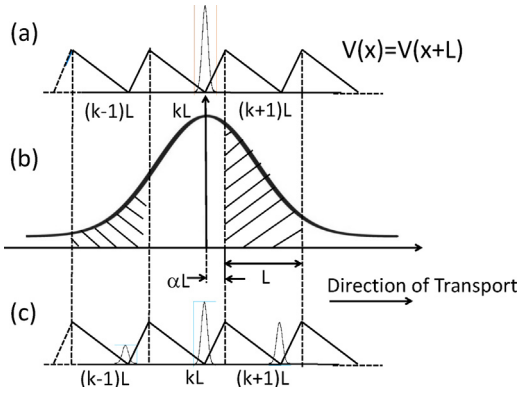

Fig. 2. (a) A periodic potential with spatial period L. (b) A Gaussian pdf with mean kL and variance t_{off}. Consider a particle which initially at time $t=0$ is at the well $x=kL$. The corresponding pdf at time $t=0$ is shown in (a). The potential is absent for time $[0, t_{off}]$. The probability of finding the particle in the region $x>(k+\alpha)L$ is much higher than finding the particle in the region $x<(k-1+\alpha L)L$ after a time t_{off}. If the potential is turned on at time t_{off} probability of having the particle move in the well at $(k+1)L$ is much higher than having the particle move to the well at $(k-1)L$ thus achieving transport to the right. (c) The evolved pdf of the particle after one flash.

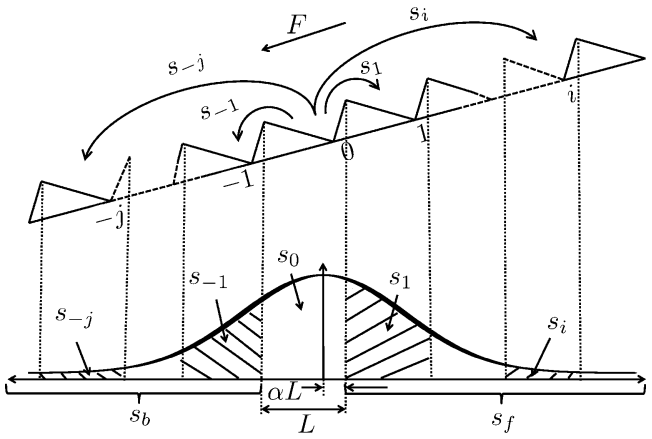

Fig. 3. Flashing ratchet showing the numbering of valleys and different transition probabilities. The valley where the particle(s) initially reside is marked as the zeroth valley. Valleys toward its right are numbered with positive integers and to the left with negative ones. The probability of jumping forward by i valleys is denoted by s_i, whereas that of jumping backwards by j valleys is denoted by s_{-j}. s_0 denotes the probability of remaining in the initial valley, while s_f and s_b denote the total probability of transportation to the front and back, respectively.

Note that the mean position of the particle remains unchanged at $x=kL$, while the variance increases linearly with time t. Thus at the end of the off-time the probability of finding the particle in the region $x>(k+\alpha)L$ and $x<(k-1+\alpha)L$ are given by $I_f = \int_{(k+\alpha)L}^{\infty} p(x, t=t_{off}|kL, 0)\,dx$ and $I_b = \int_{-\infty}^{(k-1+\alpha)L} p(x, t=t_{off}|kL, 0)\,dx$, respectively. Typically α is chosen such that the length αL is smaller than the length $(1-\alpha)L$, and therefore $I_f > I_b$. Thus upon turning the potential back on, the probability of finding the particle (using (1)) in the region $x>(k+\alpha)L$ is greater than finding it in the region $x<(k-1+\alpha)L$. The on-time t_{on} is chosen large enough to allow the particle to settle at the bottom of the well in which it is located. With these conditions, after a duration $t_{off}+t_{on}$ the particle has a higher probability of settling in the well whose minimum is at $x=(k+1)L$ or stay at the current well (at $x=kL$) than going backwards and settling in the well corresponding to $x=(k-1)L$ (the pdf of the particle's position after the potential is turned back *on* is shown in Fig. 2(c)). Thus on average, the particle moves to the right after many flashes. The above description provide the main principle exploited by Brownian Ratchets.

A specific potential that serves the requirement of Brownian Ratchets is shown in Fig. 2, which can be mathematically expressed as

$$V(x) = \begin{cases} V_0 \dfrac{\mathrm{mod}(x, L)}{\alpha L} & \text{for } \mathrm{mod}(x, L) < \alpha L \\ V_0 \left(1 - \dfrac{1}{(1-\alpha)} \left(\dfrac{\mathrm{mod}(x, L)}{L} - \alpha\right)\right) & \text{for } \mathrm{mod}(x, L) \geq \alpha L. \end{cases} \tag{2}$$

This form (see [8,13]) of potential is easily realized experimentally. Combination of all forces opposing the motion of the particle is modeled by a constant *load force* F. In biological systems, such forces may originate from intracellular mechanism [4] or sometimes from measurement devices such as optical traps [22]. In engineered systems, the load force typically is an external force [14].

The equation of motion of a particle in a thermal bath which is under the influence of a switched potential and a load force is given by the stochastic differential equation [5,20,22]

$$\gamma dx = -F dt - \theta(t) V'(x)\, dt + \sqrt{D}\, dW(t), \tag{3}$$

where γ is the viscous coefficient of the medium, $D=K_BT/\gamma$ [14] is the diffusion constant and $W(t)$ is the Wiener process. Here K_B is Boltzman's constant and T is the absolute temperature of the thermal bath. The switching parameter $\theta(t)$ is 0 when the ratchet is *off* and 1 when it is *on*.

For further analysis, we employ normalized units (n.u.) for different variables, that will make the analysis in the article applicable to a wide array of practical situations. The normalized units of different quantities are summarized in the following table.

Length	Energy	Force	Viscous coeff.	Velocity	Time
L	k_BT	$\frac{k_BT}{L}$	γ	$\frac{k_BT}{\gamma L}$	$\frac{\gamma L^2}{k_BT}$

Note that L above is the period of the ratchet potential (see Fig. 2).

3. Maximizing performance in open loop

In this section, we derive a closed form pdf of the position of the particle under the influence of a flashing ratchet with assumptions that $V_0 \gg k_BT$ and $\alpha \ll 1$ which ensure that when the potential is on, thermal noise alone can not make a particle jump from one valley (the interval $[k\alpha L, (k+1)\alpha L]$ is referred to as the kth valley) to another and at the end of the on-time, the particle is localized at the bottom of its resident valley. From the pdf, we then derive closed form expression of the mean and the variance of the transport velocity and the efficiency of transport. We also derive the conditions under which the probability of back propagation of the particle beyond a certain valley can be neglected.

Consider a particle located initially at valley 0 (see Fig. 3). The valleys to the left of valley 0 are numbered as $-1, -2, \ldots$. Similarly, to the right they are numbered as $1, 2, \ldots$. The probability of the particle jumping forward by i valleys in a single flash is denoted by s_i and that of jumping backward by j valleys is denoted by s_{-j}. Note that these probabilities are independent of the initial location of the particle.

Under the assumption of perfect localization at the resident valley during on-time, it follows that

$$s_i = P(il + \alpha L \leq x(t_{off}) \leq (i+1)L + \alpha L) \tag{4}$$

and

$$s_{-j} = P(-(j+1)L - (1-\alpha)L \leq x(t_{off}) \leq -jL - (1-\alpha)L), \tag{5}$$

where $P(a \le x \le b) = \int_a^b p(x(t_{off}), t_{off}|0,0)\,dx$ and in the presence of load force F, $p(x(t_{off}), t_{off}|0,0)$ is given by

$$p(x(t_{off}), t_{off}|0,0) = \frac{1}{\sqrt{4\pi D t_{off}}} \exp\left(-\frac{(x-(F/\gamma)t_{off})^2}{4Dt_{off}}\right). \quad (6)$$

Here, during the on-time, the particle displacements due to diffusion are neglected.

We also define the quantities $s_b = \sum_{j=1}^{\infty} s_{-j}$ and $s_f = \sum_{i=1}^{\infty} s_i$, where s_f and s_b denote the total probability of forward and backward transportation in a single flash, respectively. $s_0 = 1 - s_f - s_b$, denotes the probability of the particle remaining in the initial valley. The probability $P_k[n]$ of finding the particle in the kth valley after the nth flash is given by the master equation,

$$P_k[n] = P_k[n-1]s_0 + \sum_{i=1}^{\infty} P_{k+i}[n-1]s_{-i} + \sum_{i=1}^{\infty} P_{k-i}[n-1]s_i. \quad (7)$$

Here the first term in (7) is the probability that the particle remains in the kth valley, the second term represents the probability of the particle coming into the kth valley from valleys in front and the third term represents the probability of the particle coming into the kth valley from the valleys behind in the nth flash. As the problem is translation invariant we will assume that the particle is initially located at the zeroth valley; results hold for the initial location to be at any of the other valleys. Thus assuming $P_k[0] = \delta[k]$ (note that we have represented the dirac-delta function by $\delta(x)$ earlier; $\delta[k]$ represents the kronecker delta with $\delta[0] = 1$ and $\delta[k] = 0$ if $k \neq 0$) for all k, it follows that if we can determine s_i and s_{-i} for all i, then we can determine the probability distribution of the particle in space after any number of flashes by propagating (7).

3.1. Derivation of pdf $P_k[n]$

In this section, we present a few results that quantify bounds on backward propagation beyond a certain valley for the load force and off-time parameters that ensure forward propagation. We derive a closed form pdf for the particle propagation which are near exact solutions to (7), where the bounds obtained on forward and backward propagation significantly simplify the computation.

First we derive a bound F_{stall} on the load force that severely limits forward motion.

Theorem 1. *Let $F_{stall} := \gamma n^2 D/2\alpha L$. If load force $F > F_{stall}$, then $\sum_{i>0} s_i \le (1/2)\mathrm{erfc}(n/\sqrt{2})$ for any choice of off-time, where $\mathrm{erfc}(x) = (2/\sqrt{\pi})\int_x^{\infty} e^{-y^2}\,dy$.*

Proof. Let $F > F_{stall}$. Suppose there exists some $t_{off} = t$ such that $\sum_{i>0} s_i > (1/2)\mathrm{erfc}(n/\sqrt{2})$, then we have $\int_{\alpha L}^{\infty} (1/\sqrt{4Dt}) e^{-(((x+Ft/\gamma)^2)/4Dt)}\,dx > (1/\sqrt{\pi})\int_{n/\sqrt{2}}^{\infty} e^{-y^2}\,dy$.

Defining the variables $z = (x + Ft/\gamma)/\sqrt{2Dt}$ and $w = \sqrt{2}y$ we obtain

$$\int_{\frac{\alpha L + Ft/\gamma}{\sqrt{2Dt}}}^{\infty} e^{-z^2/2}\,dz > \int_n^{\infty} e^{-w^2/2}\,dw,$$

which implies $\alpha L + (F/\gamma)t - n\sqrt{2Dt} \le 0$. Let $g(t) := \alpha L + (F/\gamma)t - n\sqrt{2Dt}$. Note that $g(0) = \alpha L > 0$. Thus to satisfy $g(t) < 0$, we must have some $\tilde{t}$ satisfying $g(\tilde{t}) = 0$. This in turn requires that the determinant of the quadratic $\tilde{t}^2(F/\gamma)^2 + 2\tilde{t}((\alpha LF/\gamma) - n^2 D) + (\alpha L)^2 = 0$ must be greater than or equal to zero. Thus $4((\alpha LF/\gamma) - n^2 D)^2 - 4(\alpha LF/\gamma)^2 \ge 0$ which results in the inequality $F \le (\gamma n^2 D/2\alpha L) = F_{stall}$. Thus we have a contradiction to the assumptions in the theorem statement. Hence the proof follows. □

The theorem above provides an estimate of the *stalling force*. In physical systems, such as molecular motor based transport networks, that mimic Brownian ratchet mechanisms [1,12,14], stalling force is defined as the minimum value of load force beyond which no forward transport occurs for any choice of on-time and off-time.

Here n is a parameter that determines the error bound of forward propagation. For example, if $n \ge 3$, $(1/2)\mathrm{erfc}(n/\sqrt{2}) \le 0.00135$, which essentially is the mass contained beyond the 3σ tail of the Gaussian pdf. We can have a more general estimate of the stalling force if we want the forward propagation error to be less than the mass contained beyond the $n\sigma$ tail of the Gaussian distribution by choosing n to be any positive number.

Below we present conditions on t_{off} which limit forward motion.

Theorem 2. *Let load force $F < F_{stall}$ and off-time $t_{off} \notin (T_l, T_u)$, where*

$$T_l = \left(\frac{\sqrt{2Dn^2} - \sqrt{2Dn^2 - (4\alpha LF/\gamma)}}{2(F/\gamma)}\right)^2 \text{ and}$$

$$T_u = \left(\frac{\sqrt{2Dn^2} + \sqrt{2Dn^2 - (4\alpha LF/\gamma)}}{2(F/\gamma)}\right)^2.$$

Then $\sum_{i>0} s_i \le (1/2)\mathrm{erfc}(n/\sqrt{2})$, where $\mathrm{erfc}(x) = 2/\sqrt{\pi}\int_x^{\infty} e^{-y^2}\,dy$.

Proof. Let $F < F_{stall}$ and $t_{off} = t > T_u$. If $\sum_{i>0} s_i > (1/2)\mathrm{erfc}(n/\sqrt{2})$, then following the proof of Theorem 1, we have $\alpha L + (F/\gamma)t - n\sqrt{2Dt} \le 0$. Let $\beta := \sqrt{t}$ and $f(\beta) := (F/\gamma)\beta^2 - \sqrt{2Dn^2}\beta + \alpha L$ with roots $\beta_l = (\sqrt{2Dn^2} - \sqrt{2Dn^2 - (4\alpha LF/\gamma)})/(2(F/\gamma))$ and $\beta_u = (\sqrt{2Dn^2} + \sqrt{2Dn^2 - (4\alpha LF/\gamma)})/(2(F/\gamma))$. Thus, $f(\beta) \le 0$, which implies that $(\beta - \beta_l)(\beta - \beta_u) \le 0$, or $\beta \in [\beta_l, \beta_u]$. It follows that $t \in [T_l, T_u]$ which is a contradiction to the assumptions of the theorem. Similarly we can arrive at a contradiction by starting with the assumption $t_{off} = t < T_l$. Hence the proof follows. □

Definition 3. If the condition $\sum_{i>0} s_i > (1/2)\mathrm{erfc}(p/\sqrt{2})$ is satisfied for any $0 < p < 3$, then we say that the condition for **non-negligible forward transport** is met.

Corollary 4. *If load force $F < F_{stall}$ and off-time $t_{off} \in (T_l, \hat{T}_{off})$, where $\hat{T}_{off} = \alpha L/(F/\gamma)$, then the condition for non-negligible forward transport is met.*

Proof. Note that $\hat{T}_{off} < T_u$ by the inequality $\sqrt{a-b} < \sqrt{a} + \sqrt{b}$ for $a > b > 0$, and using Theorem 2. Also, $\hat{T}_{off} > T_l$ by the inequality $\sqrt{a-b} > \sqrt{a} - \sqrt{b}$ for $a > b > 0$ and using Theorem 2. The rest of the proof follows from the proof of Theorem 2. □

The theorem above together with the corollary gives us upper and lower bounds on off-time to ensure non-negligible forward transport. The lower bound on off-time in Theorem 2 is explained since the probability of the particle diffusing to the next valley is small when the off time t_{off} is small. The upper bound on off-time in Theorem 2 exists since a sufficiently large t_{off} will make the downhill drift term $(F/\gamma)t_{off}$ large enough to overwhelm the diffusion term that causes the forward transport. In either case, forward transport will be negligible. It can also be readily seen that for zero load force, we require $t_{off} > (\alpha^2 L^2/2Dp^2)$ for $0 < p < 3$ to ensure non-negligible forward transport.

Theorem 5. *If $F \in (F_m, F_{stall})$, where $F_m = (2n^2 D\gamma\alpha/((m+1-2\alpha)^2 L))$, and we ensure non-negligible forward transport, by $\sum_{i>0} s_i > (1/2)\mathrm{erfc}(p/\sqrt{2})$ for $0 \le p < 3$, by selecting off-time t such that $t \in [T_l, \hat{T}_{off}]$, then $\sum_{i<-m} s_i \le (1/2)\mathrm{erfc}(n/\sqrt{2})$, where $\mathrm{erfc}(x) = (2/\sqrt{\pi})\int_x^{\infty} e^{-y^2}\,dy$.*

Proof. Assume $F > F_m$ and $t \in [T_l, \hat{T}_{off}]$. If $\sum_{i<-m} s_i > (1/2)\mathrm{erfc}(n/\sqrt{2})$, then following the same arguments as in

previous theorems and using symmetry of normal distribution, we have $n\sqrt{2Dt} > (m+1-\alpha)L - (F/\gamma)t$. As $\hat{T}_{off} > t$, substituting $\hat{T}_{off}$ for t on both sides of the above inequality will give us $n\sqrt{2D\alpha L/(F/\gamma)} > (m+1-2\alpha)L$. It follows that $F < (2n^2 D\gamma\alpha/((m+1-2\alpha)^2 L)) = F_m$ which violates our initial assumption that $F > F_m$. Hence the proof follows. □

Theorem 5 states that if the condition of non-negligible forward transport is met, a lower bound on the value of load force would limit back propagation beyond a certain valley for all off-times that ensure non-negligible forward transport. This might seem non-intuitive at a first glance, as increasing load force is supposed to increase back propagation. The key thing to note here is, we are only interested in cases where a non-negligible forward transport takes place. A non-negligible forward transport is ensured in the form of $\hat{T}_{off}$, a maximum limit on the off-time. From Corollary 4 we can see that the maximum allowable off-time $\hat{T}_{off}$ to ensure non-negligible forward transport is a decreasing function of F. Thus, for smaller load forces, it is possible to choose a high enough off-time and still get a non-negligible forward transport. However, as this would increase the variance $2D\hat{T}_{off}$, back propagation will also be more. For higher load forces (but smaller than F_{stall}), $\hat{T}_{off}$ being small, the distribution of particles about its mean during the off-time becomes sharper, and hence back propagation beyond a certain valley can be neglected.

Theorem 6. *Let $F \in (0, F_{stall})$ and $t_{off} < \min(T_m, \hat{T}_{off})$, where*

$$T_m = \left(\frac{-\sqrt{2Dn^2} + \sqrt{2Dn^2 + ((4(m+1-\alpha)LF)/\gamma)}}{2(F/\gamma)} \right)^2.$$

If non-negligible forward transport is ensured, that is, $\sum_{i>0} s_i > (1/2)\mathrm{erfc}(p/\sqrt{2})$ for any $0 \le p < 3$, then $\sum_{i<-m} s_i \le (1/2)\mathrm{erfc}(n/\sqrt{2})$, where $\mathrm{erfc}(x) = (2/\sqrt{\pi}) \int_x^\infty e^{-y^2}\, dy$. For the case when $F = 0$, the above result holds with

$$T_m = \frac{(m+1-\alpha)L}{\sqrt{2Dn^2}}.$$

Proof. For $0 < \alpha \ll 1$, it can be shown that $T_m > T_l$ using Theorem 2. Assume $t < min(T_m, T_u)$. If $\sum_{i<-m} s_i > (1/2)\mathrm{erfc}(n/\sqrt{2})$, then following the same arguments as in previous theorems and using symmetry of the normal distribution, we have $(F/\gamma)t + n\sqrt{2Dt} - (m+1-\alpha)L > 0$.

Let $\beta := \sqrt{t}$ and $g(\beta) := (F/\gamma)\beta^2 + \sqrt{2Dn^2}\beta - (m+1-\alpha)L$. Thus, $g(\beta) > 0$ implies that $(\beta - \beta_l)(\beta - \beta_u) > 0$ where $\beta_l = (-\sqrt{2Dn^2} - \sqrt{2Dn^2 - ((4(m+1-\alpha)LF)/\gamma)})/2(F/\gamma)$ and $\beta_u = (-\sqrt{2Dn^2} + \sqrt{2Dn^2 - ((4(m+1-\alpha)LF)/\gamma)})/2(F/\gamma)$. Thus it follows that $\beta \notin [\beta_l, \beta_u]$. Now if $\beta \le \beta_l$ then $\beta^2 > \beta_u^2 \ge \min(T_m, T_u)$, which contradicts the condition $t < min(T_m, T_u)$. Hence the proof follows. □

The theorem above gives us a way to limit back propagation beyond a certain valley by controlling the off-time if the condition in Theorem 5 is not met. The condition $t_{off} < \min(T_m, \hat{T}_{off})$ ensures non-negligible forward transport in case $T_m > \hat{T}_{off}$.

From the results of Monte Carlo Simulations presented in Fig. 4, it can be seen that both forward and back propagation beyond the adjacent valley can be neglected for load forces less than the stalling force. We thus define probability of jumping one valley forward by $s_f = s_1$, probability of jumping one valley backward by $s_b = s_{-1}$ and the probability of staying in the same valley by $s_0 = 1 - s_f - s_b$. From (7), the propagation equation becomes

$$P_k[n] = s_0 P_k[n-1] + s_b P_{k+1}[n-1] + s_f P_{k-1}[n-1]. \tag{8}$$

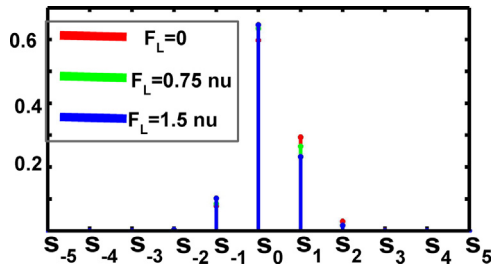

Fig. 4. The probability distribution of (forward and backward) jumping s_i of the particle in a single flash. s_i with i positive is the probability of jumping i valleys forward and with i negative is the probability of jumping i valleys backward in a single flash. s_i to different valleys in a single flash for different load forces. All simulations are done with $V_0 = 10k_BT$, $L = 1$, $\alpha = 0.1$, $\gamma = 0.1$, with different load forces and off-times that satisfy the limits of Theorems 2–5. Here all variables are presented in normalized units (n.u.).

Taking $\mathfrak{Z}$ transform over space, we obtain,

$$P_z[n] = s_0 P_z[n-1] + z s_b P_z[n-1] + z^{-1} s_f P_z[n-1], \tag{9}$$

which implies that $P_z[n] = (s_0 + z s_b + z^{-1} s_f)^n P_z[0]$.

Now, suppose initially the particle is in the zeroth well, that is, $P_k[0] = \delta[k]$, then $P_z[0] = 1$ and

$$P_z[n] = (s_0 + z s_b + z^{-1} s_f)^n. \tag{10}$$

By expanding the trinomial and collecting similar terms, we can write the coefficient of z^{-i} in the expansion to be $\sum_{\substack{p,q,r\ge 0 \\ \frac{p+q+r=n}{r-q=i}}} \binom{n}{p,q,r} s_0^p s_b^q s_f^r$, where $-n \le i \le n$.

Noting that, $\mathfrak{Z}^{-1}[z^{-i}] = \delta[k-i]$ for all $i \in \mathbb{Z}$, inverse $\mathfrak{Z}$ transform of the expansion of (10) results in,

$$P_k[n] = \sum_{\substack{p,q,r\ge 0 \\ \frac{p+q+r=n}{r-q=k}}} \binom{n}{p,q,r} s_0^p s_b^q s_f^r, \tag{11}$$

where $-n \le k \le n$ and $\binom{n}{p,q,r} = n!/p!q!r!$.

Theorem 7. *Suppose $s_b < \epsilon$, where $\epsilon > 0$ is a small parameter. Then the probability of finding the particle in the kth valley after the nth flash satisfies*

$$\binom{n}{k} s^k (1-s)^{n-k} - \gamma_1 \epsilon \le P_k[n] \le \binom{n}{k} s^k (1-s)^{n-k} + \gamma_2 \epsilon,$$

where $s_f = s$, and γ_1 and γ_2 are positive constants.

Proof. Note that (11) can be rewritten as

$$\begin{aligned} P_k[n] &= \sum_{\substack{p,r\ge 0, q=0 \\ \frac{p+r=n}{r=k}}} \binom{n}{p,r,q} s_0^p s_f^r + \sum_{\substack{p,r\ge 0, q>0 \\ \frac{p+q+r=n}{r-q=k}}} \binom{n}{p,r,q} s_0^p s_f^r s_b^q \\ &= \binom{n}{n-k,k} s_0^{n-k} s_f^k + s_b \sum_{\substack{p,r\ge 0, q>0 \\ \frac{p+q+r=n}{r-q=k}}} \binom{n}{p,r,q} s_0^p s_f^r s_b^{q-1} \\ &= \binom{n}{k} (1-s-s_b)^{n-k} s^k + s_b M \\ &\le \binom{n}{k} (1-s)^{n-k} s^k + \epsilon\gamma_2 \end{aligned},$$

where $M = \sum_{\substack{p,r\geq 0, q>0 \\ \frac{p+q+r=n}{r-q=k}}} \left(\frac{n}{p,r,q}\right) s_0^p s_f^r s_b^{q-1}$. Note that $\gamma_2 \leq P_k[n] \leq 1$ since γ_2 constitutes only a part the positive elements that sum to $P_k[n]$ in (11). This provides the upper-bound.

Now, since $M \geq 0$ (all the constituent terms of M are non-negative),

$$P_k[n] \geq \binom{n}{k}(1-s)^{n-k}\left(1+\left(-\frac{s_b}{1-s}\right)\right)^{n-k} s^k. \tag{12}$$

Since $(s_b/(1-s)) \leq 1$ and $n-k \geq 0$, applying Bernoulli's inequality [15] to (12), we obtain

$$\begin{aligned} P_k[n] &\geq \binom{n}{k}(1-s)^{n-k}\left(1-(n-k)\frac{s_b}{1-s}\right)s^k \\ &= \binom{n}{k}(1-s)^{n-k}s^k - \binom{n}{k}\left((n-k)\frac{s_b}{1-s}\right)s^k(1-s)^{n-k} \\ &= \binom{n}{k}(1-s)^{n-k}s^k - s_b Q, \end{aligned}$$

where $Q = \binom{n}{k}(n-k)s^k(1-s)^{n-k-1}$. Note that $Q \geq 0$ and bounded as $s \in [0,1]$ and $n-k \geq 0$. Thus, assuming $s_b \leq \epsilon$, we have,

$$P_k[n] \geq \binom{n}{k}(1-s)^{n-k}s^k - \gamma_2\epsilon, \tag{13}$$

where $\gamma_2 = Q$. This completes the proof. □

3.2. Derivation of velocity and efficiency

It can be seen from Fig. 4 that for low load forces, s_f is three to four times greater than s_b. Thus, in such cases, motivated by Theorem 7 if the probability of being in the kth valley after n flashes is approximated as

$$P_k[n] \approx \binom{n}{k}s^k(1-s)^{n-k}$$

then the mean position of a particle after nth flash is given by $\langle x_n\rangle = L\sum_{k=0}^{n} kP_k[n] = nLs$. Here $s = (1/\sqrt{4\pi D t_{off}})\int_{\alpha L}^{\infty}\exp(-((x-(F/\gamma)t_{off})^2/4Dt_{off}))\,dx$, which evaluates to $s = 2\,\mathrm{erfc}((\alpha L-(F/\gamma)t_{off})/\sqrt{4Dt_{off}})$. Therefore the average velocity is given by

$$\langle v_n\rangle = \langle v\rangle = \frac{nLs}{n(T_{on}+T_{off})} = \frac{Ls}{T_{on}+T_{off}}. \tag{14}$$

The variance Δv_n^2 in the velocity of the particle can be obtained as, $\langle \Delta v_n^2\rangle = (L^2 s/n(T_{on}+T_{off})^2)(1-s)$ where in the long time limit, we have, $\langle \Delta v_\infty^2\rangle = \langle \Delta v^2\rangle = 0$. We view efficiency η from an operational point of view (in contrast to the microscopic efficiency described in [14,24]), *i.e.*, $\eta = P_{out}/P_{in}$. Let P_{out} be the average rate of work done against the load force, *i.e.*, $P_{out} = Fn_p\langle v_{cm}\rangle$, where $\langle v_{cm}\rangle$ is the mean transport velocity of the center of mass of n_p particles. Clearly, for one particle, $\langle v_{cm}\rangle = \langle v\angle$. If e_f is the fraction of total run-time during which the ratchet was on, then $P_{in} = k_E e_f$, where k_E is a constant of proportionality. Thus for n_p particles, we have

$$\eta_{n_p} = \frac{P_{out}}{P_{in}} = \frac{Fn_p\langle v_{cm}\rangle}{k_E e_f}. \tag{15}$$

To avoid complications arising due to the evaluation of k_E and to normalize the efficiency irrespective of the number of particles (otherwise higher number of particles may give higher efficiency for a strategy which may not truly reflect its performance), a reference efficiency η_{ref,n_p} for n_p particles is defined and all other efficiencies with the same number of particles are scaled with respect to η_{ref,n_p}. We define η_{ref,n_p} as the efficiency achieved when an average transport velocity for the center of mass of n particles is $\langle v_{cm}\rangle = 1$ n.u. is achieved when the load force $F = 1$ n.u. and the input energy is k_E. Let the scaled efficiency be defined by

$$\eta_s = \frac{\eta_{n_p}}{\eta_{\mathrm{ref},n_p}} = \frac{F_L\langle v_{cm}\rangle}{e_f}, \tag{16}$$

where all quantities are expressed in normalized units. Clearly, η_s does not depend on the number of particles and thus is suitable for comparing the performance of different strategies.

3.3. Results and discussions

Note that the results in the previous section provide guidance on the design of flashing ratchet mechanisms. Theorems 1-5 establish bounds on experimental design parameters such as load force and off-time that result in non-negligible forward propagation. Furthermore, analytical expressions (14) and (15) can be used to guide the design of the Brownian ratchet mechanism to result in high average velocity and/or efficiency with Theorem 7 providing quantitative estimates on the accuracy of the analytical expressions obtained. We validate our analysis by comparing them against exhaustive Monte Carlo simulations. Fig. 5 depicts these results for flashing ratchet with $V_0 = 10k_BT$, $L = 1$, $\alpha = 0.1$ and $\gamma = 0.1$. The maximum average velocities plotted in red in Fig. 5(a) are obtained by running Monte Carlo simulations for 500 runs based on (3) for each load force F and each off-time $t_{\mathrm{off}} \in [T_l, \min(T_{m=0}, \hat{T}_{off})]$. For each load force F, the maximum average velocity (in blue) is then obtained by taking maximum among all the average velocities obtained over the set of off-times. In contrast the maximum average velocity (in red) for a given load force F is obtained by running Monte Carlo simulations for only *one* off-time t_{off}, which maximizes the expression for average velocity in (14). We note that there is a close agreement in the red and blue plots, which validates designing t_{off} from (14) in order to effect high-velocity transport.

Fig. 5(b) shows results for maximum efficiency, analogous to the maximum velocity case, that compares results from Monte Carlo simulations run for each off-time in an interval to the simulations done for *one* t_{off} that maximizes efficiency in (16). Thus, if a search for optimal off-time is done over a m_p point grid of off-times and n_p point grid of load force, and Monte Carlo simulation for each off-time takes t_p seconds, then using (14) and (16) would save $m_p t_p n_p$ seconds. In the simulation results presented, $m_p = 50$, $n_p = 10$ and $t_p \approx 50$ s, and thus obtaining the optimal off-time from the analytical expressions saved approximately 2.5×10^4 s. Also, the bounds on off-times from Theorems 1–6 helps limit the search space of off-times. The advantage of obtaining the optimal off-time that yields maximum velocity or efficiency in a systematic manner is important in cases where transport of large number of particles are involved (for example, colloidal self assembly [16,25]).

It should be remarked that the maximum velocity and efficiency computed using (14) and (16) shows a similar qualitative trend (not shown in the figures) as the red and blue plots; however, there is no quantitative match. The reason is that (14) ignores the back propagation term s_b and therefore average velocity (and hence efficiency) computed from (14) is higher than the case when back propagation is accounted for. However the t_{off} giving rise to maximum velocity (and efficiency) is relatively insensitive to neglecting s_b, as variation of s_b is very small around this t_{off}; thus the maximum velocity is primarily determined by the off-time that gives maximum forward transport. This is also corroborated by the results of Monte Carlo Simulations presented in Fig. 5(a) and

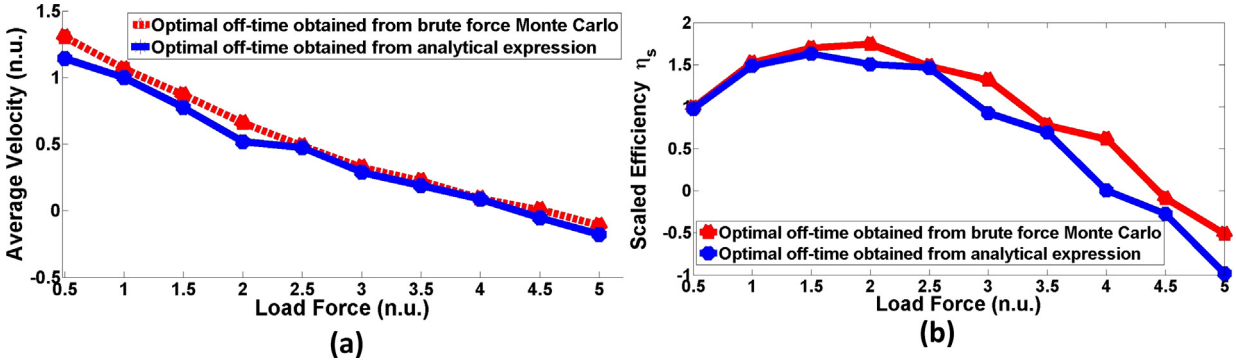

Fig. 5. (a)Maximum velocity and (b) maximum efficiency obtained in open loop for different load forces. The off-times in the red curve are obtained by brute force Monte Carlo simulations to find out which off-time gives maximum velocity and efficiency for different load forces. The off-times for maximum velocity and efficiency in the blue curve are obtained from the analytical expressions of velocity and efficiency. All simulations are done with $V_0 = 10k_BT$, $L = 1$, $\alpha = 0.1$, $\gamma = 0.1$, where all variables are presented in normalized units (n.u.).

(b) where the optimal off-times obtained from analytical results are validated by exhaustive Monte Carlo simulations.

4. Maximizing efficiency in closed loop

Under a constant load force, higher efficiency can be attempted by increasing mean velocity and/or decreasing e_f (where e_f represents the fraction of the time the ratchet potential is on). However increasing $\langle v \rangle$ and decreasing e_f can be opposing objectives since too low a e_f requires the potential to be off for most of the time which would impede achieving a high $\langle v \rangle$. Thus design of an off-time determines a trade-off between efficiency and velocity. In view of this trade-off, we pose an optimization problem that seeks the on-off time schedule to minimize a cost function that reflects both velocity and efficiency objectives. Before posing the optimization problem precisely, it is important to realize that the continuous time dynamics described by (3) will render the problem near intractable. We will now present modeling assumptions which retain the essential physics of the problem while making an optimal feedback solution determinable.

We first obtain a discrete time version of the continuous time dynamics (3). Here we assume a finite time horizon T which is divided into N stages and that a decision whether to switch the ratchet potential on or off has to be made every $T_s = T/N$ s. We denote the position $x(kT_s)$ by x_k; from (3) we have

$$\begin{aligned} x_{k+1} &= x_k - \frac{1}{\gamma}\int_{kT_s}^{(k+1)T_s} (F_L + \theta(k)V'(x))\,dt + w(k) \\ &= x_k - \frac{1}{\gamma}\int_{kT_s}^{(k+1)T_s} F_L\,dt - \int_{kT_s}^{(k+1)T_s} \theta(k)V'(x)\,dt + w(k) \\ &= x_k - \frac{F_L}{\gamma}T_s - \int_{kT_s}^{(k+1)T_s} \theta(k)V'(x)\,dt + w(k), \end{aligned} \tag{17}$$

where $\theta(k) = 1$ when potential is turned on and zero otherwise, and $w(k) \sim \mathcal{N}(0, \sqrt{2DT_s})$ is a random variable capturing the effect of thermal noise. If we represent $u_k \in \{\text{on}, \text{off}\}$ to represent the control action of turning the potential on or off at kth stage, for $u_k = \text{off}$

$$x_{k+1} = x_k - \frac{F_L}{\gamma}T_s + w(k), \tag{18}$$

and for $u_k = \text{on}$, after neglecting the effect of thermal noise (given that $V_0 \gg k_BT$),

$$x_{k+1} = x_k - \frac{F_L}{\gamma}T_s - \frac{1}{\gamma}\int_{kT_s}^{(k+1)T_s} V'(x)\,dt. \tag{19}$$

Note that for any t such that $\text{mod}(x(t), L) < \alpha L$, the force acting on the particle is negative and $V'(x(t)) = (V_0/\alpha L)$. Therefore if $mod(x(kTs), L) < \alpha L$ and T_s is small enough such that $\text{mod}(x(kT_s) - (F_L/\gamma)T_s - (V_0/\gamma\alpha L)T_s, L) < \alpha L$ with $(F_L/\gamma)T_s + (V_0/\gamma\alpha L)T_s < \alpha L$, then under the assumptions that there are negligible transient effects due to the control action at kT_s, we have $\text{mod}(x(t), L) < \alpha L$ for all $t \in [kT_s, (k+1)T_s]$. Therefore under these conditions (19) simplifies to

$$x_{k+1} = x_k - \frac{F_L}{\gamma} - \frac{V_0}{\gamma\alpha L}T_s. \tag{20}$$

Now suppose $\text{mod}(x(kTs), L) < \alpha L$ and $\text{mod}(x(kT_s) - (F_L/\gamma)T_s - (V_0/\gamma\alpha L)T_s, L) > \alpha L$ with $(F_L/\gamma)T_s + (V_0/\gamma\alpha L)T_s < \alpha L$. Then the particle will cross the valley at $L\lfloor x_k/L \rfloor$. In this case we make the approximation that at the end of time T_s, the particle is settled at $L\lfloor x_k/L \rfloor$. This assumption is justified as subsequent to the particle crossing the valley, the ratchet potential opposes its velocity and the velocity is small due to high damping. This assumption is further justified by Monte Carlo simulations (see Fig. 6(c)). Therefore, if $\text{mod}(x_k, L) < \alpha L$ and $u_k = on$,

$$x_{k+1} = \max\left(-\frac{1}{\gamma}\left(\frac{V_0}{\alpha L} + F_L\right)T_s, L\left\lfloor\frac{x_k}{L}\right\rfloor\right). \tag{21}$$

Similar approximations can be made for the case when $\text{mod}(x_k, L) > \alpha L$ and $u_k = \text{on}$. Thus, consolidating all the cases, we have the state update equation as,

$$x_{k+1} = \begin{cases} x_k - \dfrac{F_L}{\gamma}T_s + w_k & u_k = \text{off} \\ \max\left(x_k - \dfrac{1}{\gamma}\left(\dfrac{V_0}{\alpha L} + F_L\right)T_s, L\left\lfloor\dfrac{x_k}{L}\right\rfloor\right) & u_k = \text{on and} \text{mod}(x_k, L) < \alpha L \\ \min\left(x_k + \dfrac{1}{\gamma}\left(\dfrac{V_0}{1-\alpha L} - F_L\right)T_s, L\left\lceil\dfrac{x_k}{L}\right\rceil\right) & u_k = \text{on and} \text{mod}(x_k, L) \geq \alpha L. \end{cases} \tag{22}$$

The above model was reached under a series of assumptions which render the dynamics tractable. We now pose the optimization problem. Herewe do not restrict the on-off time schedule to

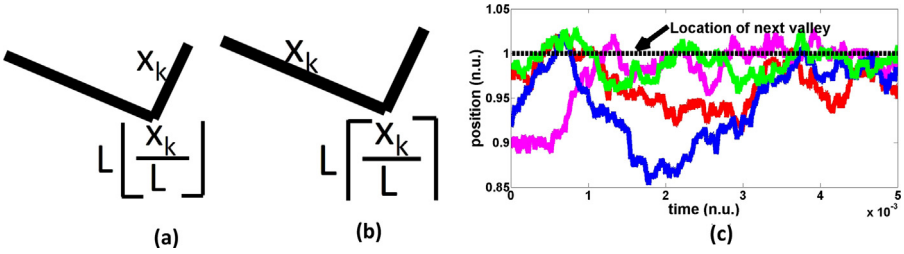

Fig. 6. The position of x_k and the valley it localizes to with the potential on when x_k is very close to the valley and is (a) on the steeper slope (b) on the gentler slope. (c) Monte Carlo simulations confirming that the particle localizes to its nearest valley with the potential on if it is located very close to it. In the simulation $T_s = 0.5$ n.u. is used and the initial position (x_k) of the particle is on the gentler slope. The black dashed line denotes the location of the next valley.

be periodic as done in Section 3; more importantly we assume that the realized *past* trajectory of the position of the particle is measured and available for determining whether to turn on or off the potential at the current time of interest. At every time instant k, the optimization problem seeks a control action $u_k \in U = \{\text{on, off}\}$, where the past positions $\{x_j\}$, $j \le k-1$ of the particle are known, that minimizes a weighted sum of input energy $\sum_{i=k}^{N-1} e_i$ to go and deviation of the *average velocity* v from v_d where $v = x_N/T$ with x_N being the final position reached when the time horizon T is reached. Here $e(k) = e$ if the potential is on at the kth instant and zero otherwise. Consider the problem of minimizing a cost function of the form

$$c_v|v_d - v| + c_e \sum_{i=k}^{N-1} e_i. \tag{23}$$

Note that a higher value of c_v/c_e emphasizes the objective of achieving the desired velocity v_d at the expense of increasing the input energy. The above objective leads to the following optimization problem:

$$\arg \min_{u_0,\ldots,u_{N-1}} \; E_{w_0,\ldots,w_{N-1}} \left[c_v|v_d - v| + c_e \sum_{i=k}^{N-1} e_i \right]. \tag{24}$$

Here, $(w_k)_{k=0}^{N-1}$ captures the effect of thermal noise at different sampling instants and thus we minimize the expected value of the cost. We cast problem (24) into a dynamic programming problem. Let the cost function $g_k(s_k, u_k, w_k)$ for stage k be,

$$g_k(x_k, u_k, w_k) = \begin{cases} c_e e & \text{for } u_k = \text{ On and } k < N \\ 0 & \text{for } u_k = \text{ Off and } k < N \\ \dfrac{1}{T} c_v |x_d - x_N| & \text{for } k = N, \end{cases} \tag{25}$$

where $x_d = v_d T$, $x_N = vT$, and $g_N(x_N)$ is the terminal cost. Thus for a initial state x_0 and a particular sequence of actions $\pi = (u_k)_{k=0}^{N-1}$, the cost of a realization with the noise sequence $(w_k)_{k=0}^{N-1}$ is

$$J_0(x_0) = g_N(x_N) + \sum_{i=0}^{N-1} g_i(x_i, u_i, w_i). \tag{26}$$

To achieve objective (24), the sequence $\pi^* = (u_k)_{k=0}^{N-1}$ that minimizes the expectation of $J_0(x_0)$ over all possible realizations of the disturbance sequence $(w_k)_{k=0}^{N-1}$ needs to be determined. Thus the following optimization problem is of interest:

$$\begin{aligned} \pi^* &= \arg \min_{\pi} \; E_{w_0,\ldots,w_{N-1}} [J_0(x_0)] \\ &= \arg \min_{\pi} \; E_{w_0,\ldots,w_{N-1}} \left[g_N(x_N) + \sum_{i=0}^{N-1} g_i(x_i, u_i, w_i) \right]. \\ &= \arg \min_{\pi} \; E_{w_0,\ldots,w_{N-1}} \left[c_v|v_d - v| + c_e \sum_{i=0}^{N-1} e_i \right]. \end{aligned} \tag{27}$$

We now analyze the dynamic programming approach [3] and the associated computational complexity to evaluate the feasibility of the method. To find a solution to the problem posed in (27), we define the cost to go $J_k^*(x_k)$ for stage k as

$$J_k^*(x_k) = \min_{u_k,\ldots,u_{N-1} w_k,\ldots,w_{N-1}} E \left[g_N(x_N) + \sum_{i=k}^{N-1} g_i(x_i, u_i, w_i) \right] \tag{28}$$

with $J_N^*(x_N) = g_N(x_N) = (1/T)c_v|x_d - x_N|$. It can be proved that [3],

$$J_k^*(x_k) = \min_{u_k \in U_{w_k}} E\,[g_k(x_k, u_k, w_k) + J_{k+1}^*(x_{k+1})]. \tag{29}$$

Thus propagating the recursion relation in (29) backwards, given $J_{k+1}^*(x_{k+1})$, we determine $J_k^*(x_k)$ for every feasible x_k using (22) and (25). This way, when we finally have $J_0^*(x_0)$, we obtain our solution π^* for optimization problem in (27).

We now provide an analysis for the computational cost. Since x_k is a real variable, the problem of computing u_k over the entire range of x_k for every stage ($1 \le k \le N-1$) is infinite dimensional. We avoid the problem of infinite dimensionality by restricting x_k to lie in a bounded set where the particle dynamics constrains the probability of x_k being outside this set to be low. Note that by using the fact that w_k follows a normal distribution with variance σ^2 in particle dynamics given in (22), we can obtain bounds d_B and d_F such that $P(d_B \le x_{k+1} - x_k < d_F) < \eta$ for any given η (also from (22) these bounds are independent of k). More specifically for $\eta = 0.95$ (that is, 95% confidence), the bounds on forward and backward travels are given by $d_F = ((V_0/\gamma(1-\alpha)L) - (F_L/\gamma))T_s + 2\sigma$ and $d_B = -((V_0/\gamma\alpha L) + (F_L/\gamma))T_s - 2\sigma$, respectively. Thus for the stage k, $x_k \in I_k = [kd_B,\ kd_F]$. Also, we grid x_k with a finite resolution $\Delta = (d_F + d_B)/m$, where m is a suitably chosen integer to control the resolution Δ. The steps above result in computing J_k^* only at a finite number of values of x_k.

For the kth stage, we need to determine $J_k^*(x_k)$ at all the km grid values of x_k. For a given x_k, two computations need to be performed to solve (29) corresponding to two actions of $u_k = $ on and $u_k = $ off and the one yielding the lower cost is chosen. There are thus $2km$ computations to be performed in evaluating (29) for the kth stage. However, as all these computations can be done independent of each other, if we have p processing units, each processing unit can perform $2km/p$ computations for the kth stage. The total number of

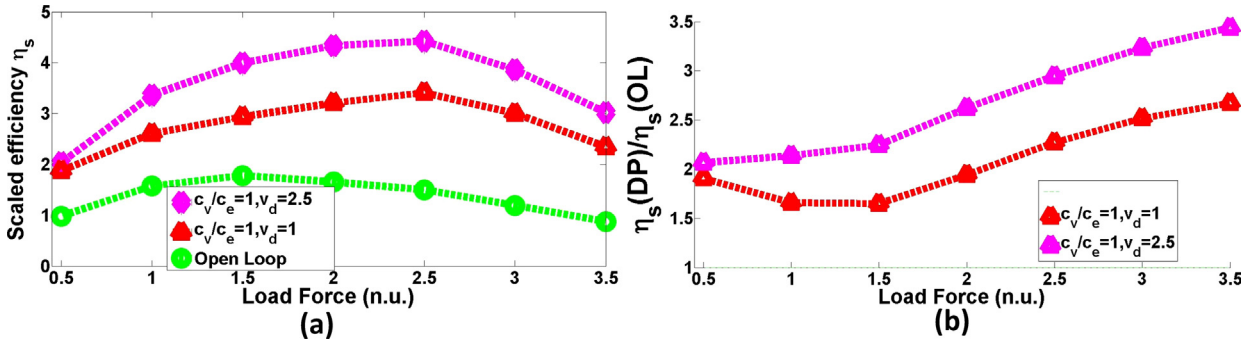

Fig. 7. Comparison of efficiency achieved at different load forces for open loop and dynamic programming. (a) shows the actual efficiencies achieved for different strategies while (b) shows the ratio of efficiency achieved of open loop strategy and dynamic programming for different optimization parameters. In (a), the green curve corresponds to open loop, red curve corresponds to dynamic programming with $c_v/c_e = 1$, $v_d = 1$ and magenta curve corresponds to dynamic programming with $c_v/c_e = 1$, $v_d = 2.5$. In (b), the red curve corresponds to the ratio $\eta_s(DP)/\eta_s(OL)$ with $c_v/c_e = 1$, $v_d = 1$ for dynamic programming and the magenta curve corresponds to $\eta_s(DP)/\eta_s(OL)$ with $c_v/c_e = 1$, $v_d = 2.5$ for dynamic programming. (For interpretation of the references to color in this figure legend, the reader is referred to the web version of the article.)

evaluations for all the stages becomes $2\sum_{k=1}^{N}(km/p) = m((N(N+1))/p)$. For modern supercomputing clusters, p and N are of the same order of magnitude and thus the computational complexity scales as N for practical conditions and hence is tractable.

4.1. Results

In this section we present the results from Monte Carlo simulations using closed-loop dynamic programming to compare its performance with open-loop approach and 'maximization of velocity' (MIV) protocol [5]. We used the same physical parameters as described in Section 3.3 for the open-loop approach. From Fig. 5 we can see that in open-loop method the maximum velocity achieved at $F_L = 3.5$ n.u. approaches zero, and thus $F_L = 3.5$ n.u. can be taken as a practical estimate of stalling force F_{stall}. Real systems are typically operated much below stalling force and hence we evaluate the performances of our strategy till F_{stall} to demonstrate its effectiveness in real scenarios.

Fig. 7 (a) and (b) shows the comparison of the open-loop and closed-loop strategies. Note that using closed-loop strategy, we can double the efficiency at low load forces while increase the efficiency more than three folds near stalling force conditions. A reason for this gain in performance is that the velocity achieved in the closed-loop, near open-loop stalling force is much greater than the open-loop strategy based velocity. It can also be seen that choosing a higher value of v_d yields better efficiency, specially at high load forces.

Fig. 8(a) and (b) compares the efficiency achieved by the MIV strategy vs that of the dynamic programming (DP) based closed-loop strategy. We can see that for low load forces DP yields approximately 35% improvement over the MIV strategy, but the effectiveness of DP decreases when load forces are increased; for high load forces, MIV outperforms DP. This may seem contradictory as DP is supposed to be optimal. However, errors introduced by finite spatial gridding and assumption of perfect localization at nearest valleys become higher for higher load forces (discussed in detail in the next section). It should also be noted that DP outperforms MIV for all load forces less than $F_{stall}/2$ which may be considered as a practical range for most realizations of Brownian ratchets.

Finally, we compare the velocity yielded by MIV and DP. From Fig. 9 we can see that for low load conditions, the velocity achieved by DP is close to the specified optimization parameter v_d. Note that the velocity achieved by MIV strategy is more than that achieved by DP. As DP yields better efficiency till $F_{stall}/2$, it corroborates our assumption that maximizing velocity does not necessarily maximize efficiency, although that seems to be the case at higher load forces.

4.2. Analysis and discussion

From the results presented in the previous section, for lower load forces DP performs significantly better in terms of efficiency, whereas for higher load forces the performance of the MIV strategy

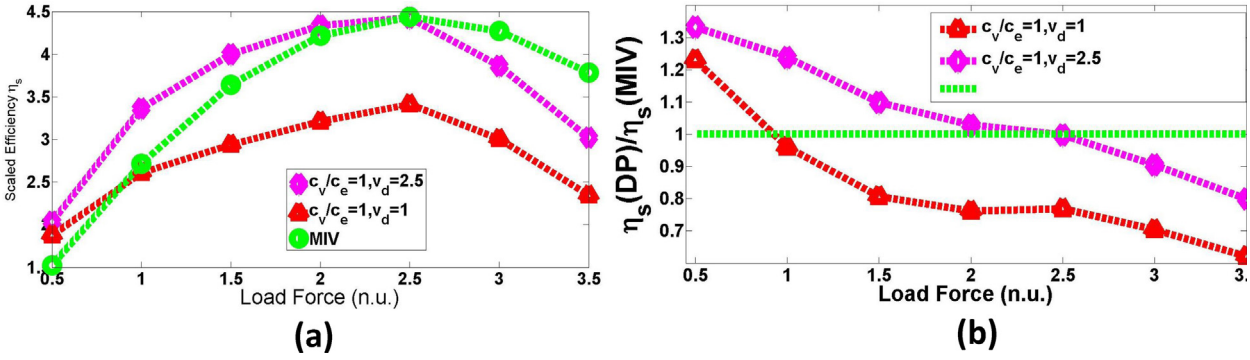

Fig. 8. Comparison of efficiency achieved at different load forces for MIV strategy and dynamic programming. (a) shows the actual efficiencies achieved for different strategies while (b) shows the ratio of efficiency achieved of MIV strategy and dynamic programming for different optimization parameters. In (a), the green curve corresponds to open loop, red curve corresponds to dynamic programming with $c_v/c_e = 1$, $v_d = 1$ and magenta curve corresponds to dynamic programming with $c_v/c_e = 1$, $v_d = 2.5$. In (b), the red curve corresponds to the ratio $\eta_s(DP)/\eta_s(MIV)$ with $c_v/c_e = 1$, $v_d = 1$ for dynamic programming, the magenta curve corresponds to $\eta_s(DP)/\eta_s(MIV)$ with $c_v/c_e = 1$, $v_d = 2.5$ for dynamic programming and the green curve corresponds to $\eta_s(DP)/\eta_s(MIV) = 1$. (For interpretation of the references to color in this figure legend, the reader is referred to the web version of the article.)

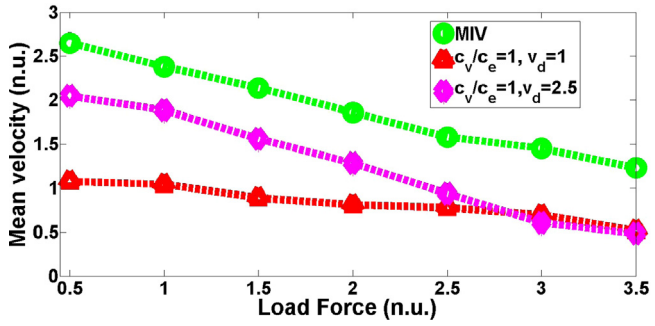

Fig. 9. Comparison of velocity achieved at different load forces for MIV strategy and dynamic programming.(green: MIV strategy, red: $c_v/c_e = 1$, $v_d = 1$, magenta: $c_v/c_e = 1$, $v_d = 2.5$). (For interpretation of the references to color in this figure legend, the reader is referred to the web version of the article.)

is very close or even outperforms DP. To understand the reason behind this, let us consider Fig. 10, where the zones are so divided that, with the potential on, if a particle starts at zone 1, it will move forward and at the end of the sampling interval it will end in zone 1 or zone 2, if a particle starts at zone 2, it will move forward and at the end of the sampling interval it will end in the adjacent valley and if a particle starts at zone 3, it will move backwards. The extent of zone 2 depends on the forward driving force $F_f = (V_0/(1-\alpha)L) - F_L$ and sampling time T_s as $\text{mod}(x_{Z2}, L) = F_f T_s$, where x_{Z2} is the starting point of zone 2. The extent of zone 1 and zone 3 then becomes clear from Fig. 10.

In the MIV strategy, if the particle is located in zone 3 at the beginning of the sampling time, the potential is turned off and if it is in either zone 1 or zone 2, it is kept on. Thus, for the instances when the particle starts at zone 2, the input energy is not fully utilized to move the particle forward, as the particle may spend considerable amount of time being stuck at the valley depending on its starting position. The dynamic programming minimizes the idle time spent at the valleys with potential turned on by looking at the global solution and scheduling when to turn on (or off) the potential with the particle at zone 2 (and also for which fraction of zone 2) and thus achieves better efficiency than the MIV strategy. It should, however, be noted that the extent of zone 2 decreases with increase in the load force F_L, which in turn decreases F_f, and thus the advantage of dynamic programming over MIV is expected to go down with increase in load force.

Since with increase in load force F_L, the backward drift during a sampling interval with potential off $x_{bw} = -(F_L/\gamma)T_s$ increases, while the forward drift with potential on $x_{fw} = (F_f/\gamma)T_s$ decreases, to achieve same forward transport, we need more on intervals or less off intervals or both. In any case, this would decrease $\langle v \rangle / e_f$ with increase in load force for same $\langle v \rangle$. If $\langle v \rangle$ is close to the maximum achievable limit, then for high enough load forces the advantage gained by keeping potential off with the particle in zone 2 may be more than offset by the negative drift suffered during that interval. Thus it can be seen from the results presented in the previous section that as the load force increases, the velocity at which maximum efficiency is achieved becomes closer to the velocity given by maximum achievable velocity. This also explains why the peak efficiency in open loop occurs at higher duty cycles for higher load forces. From the discussions in [5], it can be derived that in the limit maximum velocity is achieved for $e_{fl} := 1 - (1/\alpha)$. As discussed, higher load forces requires increase in e_f and thus our optimal strategy and MIV becomes similar in performance as $e_f \to e_{fl}$ for higher F_L.

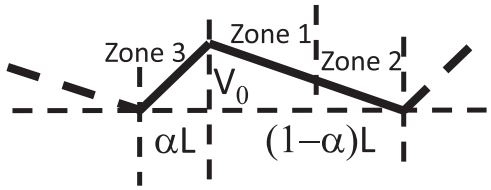

Fig. 10. Different zones on the ratchet potential based on the starting and finishing position of the particles with the potential on.

It should also be noted that the assumptions that a particle located close enough to a valley would perfectly settle in the valley with the potential on and that thermal noise can be neglected with potential on is contingent upon the fact that the barrier height V_0 is much higher than $k_B T$. However, with increase in load force, the barrier height decreases as $-F_L(1-\alpha)L$ and thus error is introduced by the state update equation (22).

Another limitation of DP stems from its implementation via spatial gridding, which in turn may be limited by the computational power available or the resolution of the position sensor. As the actions are computed recursively in dynamic programming, the error introduced due to finite spatial resolution at an early stage may be propagated among all the stages. Evidently, the penalty of such errors would be higher for higher load forces due to the increase in the negative drift term x_{bw}. The MIV strategy being a greedy strategy, the error introduced in a stage is not propagated and thus it is more robust toward spatial gridding at higher load forces. Thus, depending on the grid size Δ, coupled with the previously mentioned factors (decrease in span of zone 2, decrease in x_{fw} and increase in x_{bw} with increase in F_L), it may be possible for MIV strategy to perform better at significantly higher load forces. It should, however, be noted that this is a limitation of the implementation. Dynamic programming being an optimal strategy, if it was possible to choose an infinitesimally small grid size Δ, there would have always existed a combination of c_v, c_e, and v_d that would have performed at least as good as MIV strategy for any load force.

5. Conclusion

This article provides important guidelines for the design of Brownian ratchets operated in the open-loop mode. Specifically, this article provides bounds on the load force which if exceeded result in negligible forward transport leading to stalling of the transport for any choice of on-time and off-time schedule for the ratchet potential. In the case that the load force does not cause stalling, the viable set of on-time and off-time schedules is determined that lead to appreciable transport in the desired forward direction. Assuming a viable choice of the schedule, it is shown that backward transport of particles will be small (with quantitative estimates provided) and furthermore transport of particles beyond a certain specified distance will be small. The results above are used to estimate an approximate form of the pdf of the particle position with the error in the estimation quantified. The approximate pdf is used to devise strategies that determine the optimal schedules which maximize velocity and efficiency. Extensive Monte Carlo simulations are presented to assess the analysis which corroborate the accuracy and effectiveness of analysis.

This article also develops an optimal strategy based on dynamic programming for maximization of efficiency of transport in closed-loop. To the best of our knowledge, this is the first such strategy that maximizes efficiency in closed-loop. In comparison to open-loop methods, this strategy has shown more than two to three times improvement in terms of efficiency. Also, for lower load forces, which includes the range of the load force in majority of applications, the strategy results in 35% improvement over other closed-loop strategies that focus on velocity maximization. Thus it is demonstrated that maximizing velocity may compromise efficiency. For many particle systems assuming the particles can be

sensed, the developed closed-loop strategy can be used to maximize $\langle v_{cm} \rangle / e_f$ for a particular load force; $\langle v_{cm} \rangle$ being the average velocity of the center of mass. Methods based on approximate dynamic programming or reinforcement learning to circumvent the roadblock presented by the dimensionality of the problem are also worth considering, which constitutes our future work.

References

[1] R.D. Astumian, M. Bier, Fluctuation driven ratchets: molecular motors, Phys. Rev. Lett. 72 (March) (1994) 1766–1769.
[2] R.D. Astumian, Thermodynamics and kinetics of a brownian motor, Science 276 (5314) (1997) 917.
[3] D.P. Bertsekas, Dynamic Programming and Optimal Control, vol. 1, Athena Scientific, Belmont, 1995.
[4] M. Bier, Processive motor protein as an overdamped brownian stepper, Phys. Rev. Lett. 91 (14) (2003) 148104.
[5] F.J. Cao, L. Dinis, J.M.R. Parrondo, Feedback control in a collective flashing ratchet, Phys. Rev. Lett. 93 (2004) 040603.
[6] E.M. Craig, N.J. Kuwada, B.J. Lopez, H. Linke, Feedback control in flashing ratchets, Ann. Phys. 17 (2–3) (2008) 115–129.
[7] N.D. Derr, B.S. Goodman, R. Jungmann, A.E. Leschziner, W.M. Shih, S.L. Reck-Peterson, Tug-of-war in motor protein ensembles revealed with a programmable DNA origami scaffold, Science 338 (6107) (2012) 662–665.
[8] L.P. Faucheux, L.S. Bourdieu, P.D. Kaplan, A.J. Libchaber, Optical thermal ratchet, Phys. Rev. Lett. 74 (9) (1995) 1504.
[9] M. Feito, F.J. Cao, Time-delayed feedback control of a flashing ratchet, Phys. Rev. E 76 (December) (2007) 061113.
[10] R.P. Feynman, R.B. Leighton, M. Sands, et al., The Feynman Lectures on Physics, vol. 2, Addison-Wesley, Reading, MA, 1964.
[11] L.S.B. Goldstein, Z. Yang, Microtubule-based transport systems in neurons: the roles of kinesins and dyneins, Annu. Rev. Neurosci. 23 (1) (2000) 39–71.
[12] D. Lacoste, K. Mallick, Fluctuation theorem for the flashing ratchet model of molecular motors, Phys. Rev. E 80 (August) (2009) 021923.
[13] B.J. Lopez, N.J. Kuwada, E.M. Craig, B.R. Long, H. Linke, Realization of a feedback controlled flashing ratchet, Phys. Rev. Lett. 101 (22) (2008) 220601.
[14] H. Linke, M.T. Downton, M.J. Zuckermann, Performance characteristics of brownian motors, Chaos 15 (2) (2005) 26111.
[15] D.S. Mitrinović, J.E. Pečarić, A.M. Fink, Bernoullis inequality, in: Classical and New Inequalities in Analysis, Springer, 1993, pp. 65–81.
[16] T. Motegi, H. Nabika, K. Murakoshi, Enhanced brownian ratchet molecular separation using a self-spreading lipid bilayer, Langmuir 28 (16) (2012) 6656–6661.
[17] H. Otsuka, Y. Nagasaki, K. Kataoka, Self-assembly of poly (ethylene glycol)-based block copolymers for biomedical applications, Curr. Opin. Colloid Interface Sci. 6 (1) (2001) 3–10.
[18] P. Reimann, P. Hanggi, Introduction to the physics of brownian motors, Appl. Phys. A: Mater. Sci. Process. 75 (2002) 169–178, http://dx.doi.org/10.1007/s003390201331.
[19] E.M. Roeling, W.C. Germs, B. Smalbrugge, E.J. Geluk, T. de Vries, R.A.J. Janssen, M. Kemerink, Organic electronic ratchets doing work, Nat. Mater. 10 (1) (2011) 51–55.
[20] S. Roychowdhury, S. Salapaka, M. Salapaka, Maximizing transport in open loop for flashing ratchets, in: American Control Conference (ACC), 2012, IEEE, 2012, pp. 3210–3215.
[21] S. Roychowdhury, G. Saraswat, M.V. Salapaka, Dynamic programming based approach for optimal transport by flashing ratchet against a load force, in: Control Applications (CCA), 2013 IEEE International Conference on, IEEE, 2013, pp. 1105–1110.
[22] S. Salapaka, S. Roychowdhury, M. Salapaka, Modeling and role of feedback controlled stochastic ratchets in cellular transport, in: Decision and Control (CDC), 2012 IEEE 51st Annual Conference on, IEEE, 2012, pp. 374–379.
[23] N. Stephanopoulos, E.O.P. Solis, G. Stephanopoulos, Nanoscale process systems engineering: toward molecular factories synthetic cells and adaptive devices, AIChE J. 51 (7) (2005) 1858–1869.
[24] D. Suzuki, T. Munakata, Rectification efficiency of a brownian motor, Phys. Rev. E 68 (2) (2003) 021906.
[25] A. Van Oudenaarden, S.G. Boxer, Brownian ratchets: molecular separations in lipid bilayers supported on patterned arrays, Science 285 (5430) (1999) 1046–1048.
[26] K.J. Verhey, N. Kaul, V. Soppina, Kinesin assembly and movement in cells, Annu. Rev. Biophys. 40 (2011) 267–288.
[27] A.J.M. Wollman, C. Sanchez-Cano, H.M.J. Carstairs, R.A. Cross, A.J. Turberfield, Transport and self-organization across different length scales powered by motor proteins and programmed by DNA, Nat. Nanotechnol. (2013).